

Joint Active and Passive Beamforming for RIS-aided MIMO Communications with Low-Resolution Phase Shifts

Nuno Souto, *Senior Member, IEEE*

Abstract— In recent years, reconfigurable intelligent surface (RIS) has emerged as an appealing technology due to its potential capability to enhance the performance of wireless networks with a low-cost and low energy-consumption. Most works often assume continuous phase-shifts at the RIS elements for the transmit and passive beamforming optimization. However, practical hardware limitations often impose a reduced number of available phase shifts at the RIS elements which can lead to substantial performance loss. Therefore, to harvest the gains of RIS-assisted multi-stream multiple-input multiple-output (MIMO) communications under the constraint of discrete-valued phases shifts, this correspondence proposes an iterative algorithm that can efficiently tackle the mixed integer non-linear optimization problem associated to the maximization of the achievable rate over the transmit precoder and RIS elements. Simulation results demonstrate that the proposed design can be very effective, especially when using low-resolution phase-shifts.

Index Terms—Reconfigurable intelligent surface (RIS), multiple-input multiple-output (MIMO), optimization, discrete phase shifts.

I. INTRODUCTION

At a time when the fifth generation (5G) of mobile communications networks is being rolled out around the world, research efforts are already underway to develop the technologies that will incorporate the future sixth generation of wireless systems. In fact, with the advent of demanding applications such as virtual/augmented reality, holographic projection, autonomous driving and tactile Internet, it is clear that full support will only be possible in 6G [1]. One of the key technologies that is expected to help address the challenges in 6G networks corresponds to reconfigurable intelligent surfaces (RISs) [2]. RIS are artificial planar surfaces comprising a large number of reconfigurable elements that can be programmed to manipulate incident electromagnetic waves at a very high spatial resolution. This allows the implementation of non-conventional functionalities such as wave steering, focusing, imaging, and holography [3]. Therefore, RIS can be used for improving overall system performance, for example by reducing interference or extending signal coverage which is critical when operating in the higher frequency bands

envisioned for 6G (mmWave and THz) [4]. A RIS is thus an enabler for the realization of smart wireless environments where the wireless channel becomes part of the network design parameters, which can be optimized alongside the transmitter and receiver [5].

Due to its appealing features, RIS has attracted extensive research work in recent years, as summarized in [6]. In particular, several works have focused on the optimization of both the transmit and passive beamforming [7]- [10]. Since the joint optimization problem is challenging, a few simplified approaches where the transmit precoder and RIS elements are independently optimized have been proposed, as in [7]. While this may reduce the implementation complexity, the performance can be improved by adopting a joint design. Therefore, the work in [8] considered a single-user multiple-input single-output (MISO) communication channel and proposed a branch-and-bound algorithm that can find global optimal solutions for both the active and passive beamformers when the objective is to maximize the spectral efficiency. Due to the extremely high computational complexity associated to finding global optimal solutions, most approaches propose suboptimal algorithms. In [9] the authors proposed an iterative algorithm based on the projected gradient method (PGM) which maximizes the achievable rate over the transmit covariance matrix and RIS phases. In [10] the authors addressed a simplified formulation based on the sum of gains maximization criterion which is solved using the alternating direction method of multipliers for obtaining the RIS followed by the singular value decomposition for computing the precoder.

All the previous works assumed continuous phase shifts at the RIS elements for the design of the algorithms. Realizing hardware that can support continuous tuning of the phases of the individual RIS elements can be prohibitively expensive and unfeasible, especially when the number of elements is large [11]. Therefore, practical RISs often operate with a reduced number of phase shifts [12]. The simplest approach to cope with finite resolution phase shifts is to directly quantize the solutions obtained with a continuous based algorithm to the nearest discrete values, as adopted in the PGM based approach in [9]. While simple to implement, this rounding method can result in significant performance degradation, especially with low-resolution phase shifts [13]. Therefore, some recent works have considered the discrete-valued phase shifts constraint directly inside the precoder and RIS optimization. In [12], the authors

This work is funded by FCT/MCTES through national funds and when applicable co-funded by EU funds under the project UIDB/50008/2020.

N. Souto is with the ISCTE-University Institute of Lisbon and Instituto de Telecomunicações, 1649-026 Lisboa, Portugal (e-mail: nuno.souto@lx.it.pt).

considered a MISO scenario and represented the joint optimization problem as a linear program with binary variables. To find the optimal global solution, they applied the branch-and-bound method which has exponential computational complexity. The authors in [14] presented an algorithm that computes the optimal beamforming vector for any discrete phase resolution. Although having low complexity, the approach was designed for single-antenna transmitters and receivers. A different approach was followed in [15], where particle swarm optimization was applied as a heuristic method for rate maximization in scenarios with multiple single-antenna users, considering both continuous and discrete phase-shifts.

Motivated by the work above, in this correspondence we study a multi-stream MIMO system where a RIS with a limited number of phase shifts helps to establish the communication between a transmitter and a receiver. Specifically, the main contributions of the paper can be summarized as follows:

- Aiming at the maximization of the achievable rate, the transmit precoder and the RIS are jointly optimized under the assumption of discrete-valued phase shifts. To cope with the resulting mixed-integer non-linear program (MINLP) whose optimal solution can be difficult to find, we reformulate it using the convex hull of the discrete phase shifts.
- We apply the cyclic block proximal gradient (CBPG) method for optimizing the precoder and RIS, combined with an extrapolation step in the update of the individual variables in order to accelerate the convergence speed. This allows us to obtain an iterative algorithm comprising a sequence of simple projections.
- Through numerical simulations, we evaluate the performance of the proposed approach and show that it can be very effective, especially when low-resolution phase shifters are assumed at the RIS.

The rest of the paper is organized as follows. Section II defines the system model whereas section III formulates the joint precoder and RIS optimization problem and describes the proposed algorithm to solve it. Section IV presents numerical performance results followed by the conclusions in section V.

Notation: Matrices and vectors are represented by uppercase and lowercase boldface letters, respectively. $(\cdot)^T$ and $(\cdot)^H$ denote the transpose and conjugate transpose, $\|\cdot\|_2$ is the 2-norm of a vector/matrix, $\|\cdot\|_F$ is the Frobenius norm, $\text{vec}(\cdot)$ is the vectorization operator which is a vector obtained by stacking the columns of the argument matrix, $\text{diag}(\cdot)$ transforms a vector into a diagonal matrix or represents the diagonal of a matrix, \mathbf{I}_n is the $n \times n$ identity matrix and $\mathcal{I}_{\mathcal{D}}(\mathbf{v})$ is the indicator function which returns 0 if $\mathbf{v} \in \mathcal{D}$ and $+\infty$ otherwise.

II. SYSTEM MODEL

Let us consider the MIMO communication system illustrated in Fig. 1, where a transmitter equipped with N_{tx} antennas sends N_s simultaneous data streams to a receiver with N_{rx} antennas, with the aid of a RIS panel comprising N_{ris} elements.

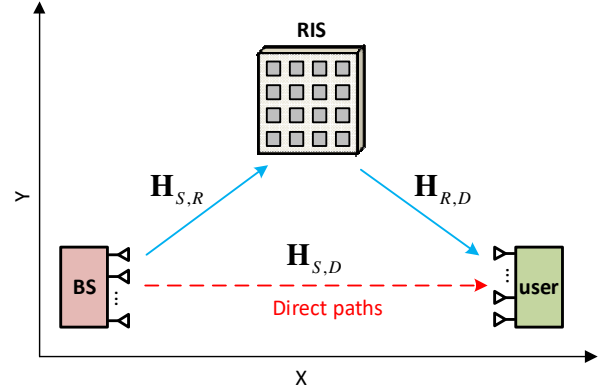


Fig. 1. System model layout considered for the multi-stream RIS-assisted MIMO communication system.

Representing the transmitted signal as $\mathbf{s} = [s_1 \dots s_{N_s}]^T$, where $s_i \in \mathbb{C}$ is an amplitude and phase modulated symbol with $\mathbb{E}[\|\mathbf{s}\|_2^2] = N_s$, then the received signal can be expressed as

$$\mathbf{r} = \sqrt{\rho} \mathbf{H} \mathbf{F} \mathbf{s} + \mathbf{n}, \quad (1)$$

where $\sqrt{\rho}$ is the power per stream, $\mathbf{H} \in \mathbb{C}^{N_{rx} \times N_{tx}}$ is the channel matrix and $\mathbf{F} \in \mathbb{C}^{N_{tx} \times N_s}$ is the precoder matrix. Vector $\mathbf{n} \in \mathbb{C}^{N_{rx} \times 1}$ contains random noise samples distributed according to $\mathcal{CN}(\mathbf{0}, \sigma_n^2 \mathbf{I}_{N_{rx}})$. Matrix \mathbf{H} can be written as

$$\mathbf{H} = \mathbf{H}_{S,D} + \mathbf{H}_{R,D} \mathbf{\Phi} \mathbf{H}_{S,R}, \quad (2)$$

where $\mathbf{H}_{S,D} \in \mathbb{C}^{N_{rx} \times N_{tx}}$ represents the direct channel between the transmitter and receiver, $\mathbf{H}_{S,R} \in \mathbb{C}^{N_{ris} \times N_{tx}}$ is the channel between the transmitter and the RIS and $\mathbf{H}_{R,D} \in \mathbb{C}^{N_{rx} \times N_{ris}}$ is the channel between the RIS and the receiver. $\mathbf{\Phi} \in \mathbb{C}^{N_{ris} \times N_{ris}}$ is the phase shift matrix of the RIS which has a diagonal structure namely, $\mathbf{\Phi} = \text{diag}(\boldsymbol{\varphi})$ with $\boldsymbol{\varphi} = [\varphi_1, \dots, \varphi_{N_{ris}}]^T$. Assuming discrete phase shifts with N_b quantization bits then we can represent the elements of the RIS matrix as $\varphi_i \in \left\{ a e^{j \frac{2\pi k}{M}} : k = 0, \dots, M-1 \right\}$, $i = 1, \dots, N_{ris}$, where a denotes the amplitude of the reflection coefficients and $M = 2^{N_b}$ is the number of possible phase shifts.

III. PROBLEM FORMULATION AND ALGORITHM DESCRIPTION

A. Achievable Rate Maximization with Discrete Constraints

Assuming Gaussian signaling and perfect channel knowledge, we can express the achievable rate as [9]

$$R = \log_2 \det \left(\mathbf{I}_{N_s} + \frac{\rho}{P_n} \mathbf{F}^H \mathbf{H}^H \mathbf{H} \mathbf{F} \right) \text{ (bits/s/Hz)}, \quad (3)$$

where P_n is the noise power (i.e., $P_n = \sigma_n^2$). The joint rate maximization problem can be written as

Algorithm 1: DA-CBPG Algorithm

- 1: **Input:** $\mathbf{r}, \mathbf{H}, \alpha, Q, \mathbf{F}^{(0)}, \mathbf{t}^{(0)}$
 - 2: $\mathbf{F}^{(1)} = \mathbf{F}^{(0)}, \mathbf{t}^{(1)} = \mathbf{t}^{(0)}$
 - 3: **for** $q=1, \dots, Q$ **do**
 - 4: $\mathbf{P}^{(q)} = \mathbf{F}^{(q)} + \frac{q}{q+3}(\mathbf{F}^{(q)} - \mathbf{F}^{(q-1)})$
 - 5: $\mathbf{F}^{(q+1)} = \text{prox}_{\alpha \mathcal{Z}_c} \left(\mathbf{P}^{(q)} - \alpha \nabla_{\mathbf{F}^*} f \left(\mathbf{P}^{(q)}, (\mathbf{I}_{N_{rs}} \otimes \boldsymbol{\theta}^T) \mathbf{t}^{(q)} \right) \right)$
 - 6: $\mathbf{y}^{(q)} = \mathbf{t}^{(q)} + \frac{q}{q+3}(\mathbf{t}^{(q)} - \mathbf{t}^{(q-1)})$
 - 7: $\mathbf{t}^{(q+1)} = \text{prox}_{\alpha \mathcal{Z}_D} \left(\mathbf{y}^{(q)} - \alpha \nabla_{\mathbf{t}} f \left(\mathbf{F}^{(q+1)}, (\mathbf{I}_{N_{rs}} \otimes \boldsymbol{\theta}^T) \mathbf{y}^{(q)} \right) \right)$
 - 8: **end for**
 - 9: **Output:** $\mathbf{F}^{(q+1)}, \boldsymbol{\varphi} = (\mathbf{I}_{N_{rs}} \otimes \boldsymbol{\theta}^T) \mathbf{t}^{(q+1)}$.
-

$$\min_{\substack{\mathbf{F} \in \mathbb{C}^{N_{rx} \times N_s} \\ \boldsymbol{\varphi} \in \mathbb{C}^{N_{rs} \times M}}} f(\mathbf{F}, \boldsymbol{\varphi}) = -\ln \det \left(\mathbf{I}_{N_s} + \frac{\rho}{P_n} \mathbf{F}^H \mathbf{H}^H \mathbf{H} \mathbf{F} \right) \quad (4a)$$

$$\text{subject to } \|\mathbf{F}\|_F^2 \leq N_s \quad (4b)$$

$$\boldsymbol{\varphi}_i \in \left\{ a e^{j \frac{2\pi k}{M}} : k=0, \dots, M-1 \right\}, i=1, \dots, N_{rs}. \quad (4c)$$

This formulation is nonconvex due to the coupling between \mathbf{F} and $\boldsymbol{\varphi}$ in (4a), which, combined with the discrete constraint (4c), results in a nonconvex MINLP. Therefore, finding a global solution efficiently is difficult. To cope with the discrete restriction, we can relax (4c) using the convex hull of the discrete phase shifts. To accomplish this, we first rewrite (4c) in an equivalent form, namely as

$$\boldsymbol{\varphi}_i = \sum_{k=0}^{M-1} t_{i,k} \boldsymbol{\theta}_k, t_{i,k} \in \{0, 1\}, \sum_{k=0}^{M-1} t_{i,k} = 1 \quad (5)$$

with $\boldsymbol{\theta}_k = a e^{j \frac{2\pi k}{M}}$ and $t_{i,k} \in \mathbb{R}$. We can then relax the second condition in (5) to $t_{i,k} \geq 0$ and rewrite (5) as

$$\boldsymbol{\varphi}_i = \mathbf{t}_i^T \boldsymbol{\theta}, \mathbf{t}_i \geq 0, \mathbf{t}_i^T \bar{\mathbf{1}} = 1, \quad (6)$$

where $\boldsymbol{\theta} = [\boldsymbol{\theta}_0, \dots, \boldsymbol{\theta}_{M-1}]^T$, $\mathbf{t}_i = [t_{i,0}, \dots, t_{i,M-1}]^T$ ($i=1, \dots, N_{rs}$), $\bar{\mathbf{1}}$ denotes the all-ones vector. Using this convex set constraint and defining $\mathbf{T} = [\mathbf{t}_1, \dots, \mathbf{t}_{N_{rs}}]^T$ and $\mathbf{t} = \text{vec}(\mathbf{T}^T)$, we can express optimization problem (4) as

$$\min_{\substack{\mathbf{F} \in \mathbb{C}^{N_{rx} \times N_s} \\ \mathbf{T} \in \mathbb{R}^{N_{rs} \times M}}} f(\mathbf{F}, \mathbf{T}\boldsymbol{\theta}) + \mathcal{Z}_c(\mathbf{F}) + \mathcal{Z}_D(\mathbf{t}), \quad (7)$$

with $\mathcal{C} = \left\{ \mathbf{X} \in \mathbb{C}^{N_{rx} \times N_s} : \|\mathbf{X}\|_F^2 \leq N_s \right\}$ and

$$\mathcal{D} = \left\{ \mathbf{b} \in \mathbb{R}^{MN_{rs}} : \mathbf{b} \geq 0, \mathbf{b}_i^T \bar{\mathbf{1}} = 1 \right\}.$$

B. Proposed Algorithm

To address problem (7), we apply the CBPG method [16] by optimizing and updating matrices \mathbf{F} and \mathbf{T} in turn, keeping the other variable fixed. Each update consists of a gradient-based

step, followed by a proximal mapping, defined as

$$\text{prox}_{\alpha g}(\mathbf{a}) = \underset{\hat{\mathbf{x}}}{\text{argmin}} g(\hat{\mathbf{x}}) + \frac{1}{2\alpha} \|\hat{\mathbf{x}} - \mathbf{a}\|_2^2. \quad (8)$$

for a function g . Instead of computing the gradient steps over the previous points, $\mathbf{F}^{(q)}$ and $\mathbf{t}^{(q)}$ (q is the iteration number), we use extrapolated points, $\mathbf{P}^{(q)}$ and $\mathbf{y}^{(q)}$, which are linear combinations of the previous two estimates, as these can improve the typical slow convergence of proximal gradient methods, as discussed in [17]. The overall discrete accelerated CBPG based (DA-CBPG) algorithm is summarized in Algorithm 1. Q denotes the maximum number of iterations and α is the step size, which can be found through backtracking line search [18]. The proximal mapping in step 5 reduces to the Euclidean projection over \mathcal{C}

$$\text{prox}_{\alpha \mathcal{Z}_c}(\mathbf{X}) = \begin{cases} \mathbf{X}, & \|\mathbf{X}\|_F^2 \leq N_s \\ \frac{\sqrt{N_s}}{\|\mathbf{X}\|_F} \mathbf{X}, & \text{otherwise} \end{cases}. \quad (9)$$

Step 7 can be expressed as $\text{prox}_{\alpha \mathcal{Z}_D}(\mathbf{x}) = \left[\Pi_S(\mathbf{x}_1)^T \dots \Pi_S(\mathbf{x}_{N_{rs}})^T \right]^T$, where $\Pi_S(\cdot)$ is the projection over the probability simplex ([17], section 6.2), i.e.,

$$\Pi_S(\mathbf{x}_i) = (\mathbf{x}_i - v_i \bar{\mathbf{1}})_+, \quad (10)$$

where v_i is the value that satisfies $\bar{\mathbf{1}}^T (\mathbf{x}_i - v_i \bar{\mathbf{1}})_+ = 1$, with $(\cdot)_+$ defined as $(a)_+ = \max(a, 0)$. The algorithm in [19] can be used for computing (10) efficiently. The gradients required for steps 5 and 7 are computed according to the following lemma:

Lemma 1: Let $f(\mathbf{F}, \boldsymbol{\varphi})$ be defined as in (4a), where the channel matrix is represented as (2) with $\boldsymbol{\varphi} = (\mathbf{I}_{N_{rs}} \otimes \boldsymbol{\theta}^T) \mathbf{t}$.

Then, the gradients with respect to \mathbf{F}^* and \mathbf{t} can be obtained as

$$\nabla_{\mathbf{F}^*} f(\mathbf{F}, \boldsymbol{\varphi}) = -\frac{\rho}{P_n} \mathbf{H}^H \mathbf{H} \mathbf{F} \left(\mathbf{I}_{N_s} + \frac{\rho}{P_n} \mathbf{F}^H \mathbf{H}^H \mathbf{H} \mathbf{F} \right)^{-1} \quad (11)$$

and

$$\nabla_{\mathbf{t}} f(\mathbf{F}, (\mathbf{I}_{N_{rs}} \otimes \boldsymbol{\theta}^T) \mathbf{t}) = -2 \text{Re} \left\{ \text{vec}(\boldsymbol{\theta} \text{diag}^T(\mathbf{Z})) \right\}, \quad (12)$$

with

$$\mathbf{Z} = \mathbf{H}_{S,R} \mathbf{F} \left(\mathbf{I}_{N_s} + \frac{\rho}{P_n} \mathbf{F}^H \mathbf{H}^H \mathbf{H} \mathbf{F} \right)^{-1} \mathbf{F}^H \mathbf{H}^H \mathbf{H}_{R,D}. \quad (13)$$

Proof: Proof is shown in Appendix A.

IV. NUMERICAL RESULTS

In this section we provide numerical results which were obtained using Monte Carlo simulations. We consider a multi-stream MIMO communication with $N_s=2$, $N_{rx}=64$, $N_{rs}=16$. The transmitter, receiver and RIS are located at (0,0) m, (50,0) m and (40,10) m, respectively (the third dimension is assumed to be the same for all). We consider that the amplitude of the reflection coefficients is $a=1$, with the operating frequency set

to 28 GHz and the bandwidth to 800 MHz. In the simulations we adopt a clustered geometric channel model [20] where the transmitter-RIS and RIS-receiver links have one line-of-sight (LOS) and N_{ray} non line-of-sight (NLOS) components. The channel between transmitter and RIS can be expressed as

$$\mathbf{H}_{S,R} = \sqrt{\beta_{LOS}^{S,R}} e^{-j2\pi d_{S \leftrightarrow R} / \lambda} \mathbf{a}_R(\phi_0^{R \leftarrow S}, \theta_0^{R \leftarrow S}) \mathbf{a}_S(\phi_0^{S \rightarrow R}, \theta_0^{S \rightarrow R})^H + \sqrt{\frac{\beta_{NLOS}^{S,R}}{K_{Rice}}} \sum_{l=1}^{N_{ray}} \alpha_l^{S,R} \mathbf{a}_R(\phi_l^{R \leftarrow S}, \theta_l^{R \leftarrow S}) \mathbf{a}_S(\phi_l^{S \rightarrow R}, \theta_l^{S \rightarrow R})^H, \quad (14)$$

where λ is the wavelength, $d_{S \leftrightarrow R}$ is the distance between the BS and the RIS, $\alpha_l^{S,R}$ is the complex gain of the l^{th} path (with $\sum_{l=1}^{N_{ray}} E[|\alpha_l^{S,R}|^2] = 1$) and K_{Rice} defines the energy ratio between the LOS and NLOS components. $\beta_{NLOS}^{S,R}$ represents the path loss which is given by

$$\beta_{NLOS}^{S,R} = \frac{G_{tx} A_{RIS}}{4\pi (d_{S \leftrightarrow R})^\gamma} e^{-k_{abs}(f) d_{S \leftrightarrow R}}, \quad (15)$$

where G_{tx} is the transmit antenna gain, A_{RIS} is the area of a RIS element, γ is the path loss exponent and $k_{abs}(f)$ is the molecular absorption coefficient at frequency f . $\mathbf{a}_S(\phi_l^{S \rightarrow R}, \theta_l^{S \rightarrow R})$ and $\mathbf{a}_R(\phi_l^{R \leftarrow S}, \theta_l^{R \leftarrow S})$ denote the array response at the transmitter and RIS, at the pair of azimuth and elevation angles of departure (AoD) and arrival (AoA) of $(\phi_l^{S \rightarrow R}, \theta_l^{S \rightarrow R})$ and $(\phi_l^{R \leftarrow S}, \theta_l^{R \leftarrow S})$. In the simulations, square uniform planar arrays (UPAs) are used, whose steering vectors are given by

$$\mathbf{a}_S(\phi_l^{S \rightarrow R}, \theta_l^{S \rightarrow R}) = \begin{bmatrix} 1, \dots, e^{j\frac{2\pi}{\lambda} d_S (p \sin \phi_l^{S \rightarrow R} \sin \theta_l^{S \rightarrow R} + q \cos \theta_l^{S \rightarrow R})}, \\ \dots, e^{j\frac{2\pi}{\lambda} d_S ((\sqrt{N_{tx}}-1) \sin \phi_l^{S \rightarrow R} \sin \theta_l^{S \rightarrow R} + (\sqrt{N_{tx}}-1) \cos \theta_l^{S \rightarrow R})} \end{bmatrix}^T, \quad (16)$$

with $0 \leq p, q < \sqrt{N_{tx}}$ and d_S denoting the inter-element spacing, which in the simulation is set as $\lambda/2$. $\mathbf{H}_{R,D}$ and $\mathbf{H}_{S,D}$ are defined using similar expressions but for the later we assume that no LOS path exists due to surrounding obstructions. In the following results we apply a path loss exponent of 1.90 for the LOS propagation and 4.39 for the NLOS propagation [21]. Furthermore, we use $K_{Rice}=10$ for the indirect link and $N_{ray}=10$, with the azimuth and elevation AoD/AoA uniformly random distributed in $[-\pi, \pi)$ and $[-\frac{\pi}{2}, \frac{\pi}{2})$, respectively. All the results are averaged over 1000 random channel realizations.

Fig. 2 shows the achievable rate versus the number of RIS elements obtained with the proposed approach using one quantization bit only. Curves obtained with no RIS, a static RIS, the RIS-only APG algorithm (R-APG) from [7] and the PGM algorithm [9] are included as benchmarks. It can be seen that in this scenario, the use of a properly optimized RIS can provide substantial gains over a communication without RIS. Still, R-

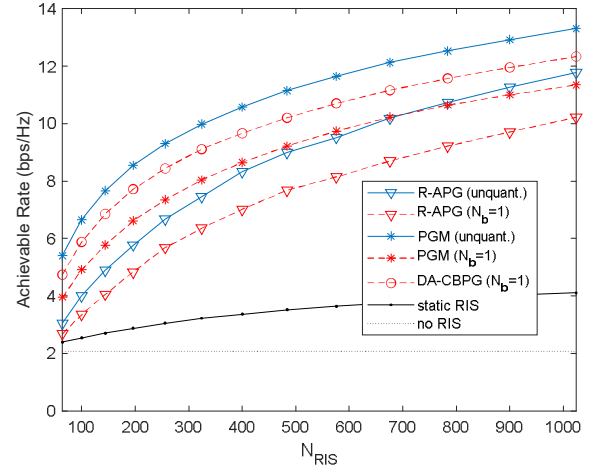


Fig. 2. Achievable rate versus number of RIS elements (N_{ris}) with different algorithms. Scenario with: $N_s=2$, $N_{tx}=64$, $N_{rx}=16$ and $P_{tx}=30$ dBm.

APG has the worst performance as it only optimizes the RIS matrix after the precoder is defined. Conversely, PGM and DA-CBPG perform joint optimization of the precoder and RIS and can achieve higher rates. It is also clear that a substantial performance degradation occurs when phase shifters with only one bit resolution are used. Still, the proposed DA-CBPG is able to provide the closest rates to the best unquantized case.

Fig. 3 evaluates the impact of the number of quantization bits on the achievable rate of the different approaches when $N_{ris}=196$. As expected, it can be observed that compared to the unquantized case, the highest rate degradation occurs when the number of quantization bits is low. However, the proposed DA-CBPG approach can significantly reduce the degradation, especially when $N_b=1$, and with $N_b=3$ it can even slightly outperform unquantized PGM.

V. CONCLUSIONS

This paper addressed the problem of maximizing the achievable rate jointly over the transmit precoder and RIS elements, considering multi-stream MIMO communications with realistic discrete phase-shifts. It was shown that the resulting problem renders a nonconvex MINLP, whose optimal solution generally cannot be found efficiently. Therefore, we reformulated the problem, approximating the discrete-valued phase shifts constraint with the convex hull, upon which we could then apply the CBPG method combined with an extrapolation step. This allowed us to derive an iterative algorithm comprising a sequence of simple projections. Numerical results showed that the proposed approach can reduce the performance loss incurred with the use of low-resolution phase shifts at the RIS, achieving higher rates than other benchmarked schemes.

APPENDIX A

PROOF OF LEMMA 1

In the following we apply the procedure described in [22]. For obtaining the complex-valued gradient of $f(\mathbf{F}, \boldsymbol{\varphi})$ with respect to \mathbf{F}^* , we write the complex differential as

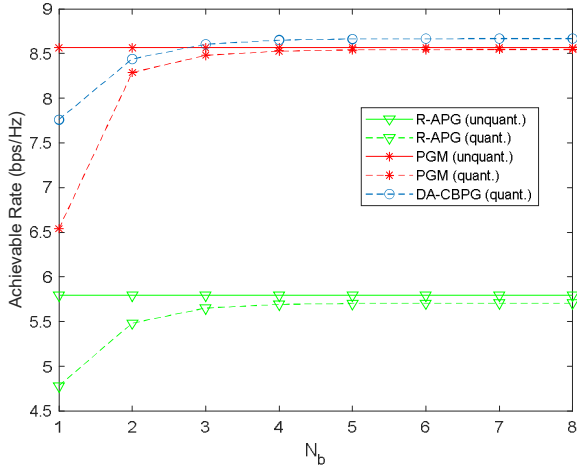


Fig. 3. Achievable rate versus number of quantization bits (N_b) for the phase shifts with different algorithms. Scenario with: $N_s=2$, $N_r=64$, $N_{rs}=16$, $N_{ris}=196$ and $P_n=30$ dBm.

$$df = -\text{Tr} \left\{ \frac{\rho}{P_n} \left(\mathbf{I}_{N_s} + \frac{\rho}{P_n} \mathbf{F}^H \mathbf{H}^H \mathbf{H} \mathbf{F} \right)^{-1} \times \left(\mathbf{F}^H \mathbf{H}^H \mathbf{H} \mathbf{d} \mathbf{F} + d \mathbf{F}^H \mathbf{H}^H \mathbf{H} \mathbf{F} \right) \right\}. \quad (17)$$

Applying the relation $d(\ln \det(\mathbf{X})) = \text{Tr}\{\mathbf{X}^{-1} d\mathbf{X}\}$ ([22], Table 3.1) we can rewrite the differential as

$$df = -\text{Tr} \left\{ \frac{\rho}{P_n} \left(\mathbf{I}_{N_s} + \frac{\rho}{P_n} \mathbf{F}^H \mathbf{H}^H \mathbf{H} \mathbf{F} \right)^{-1} \mathbf{F}^H \mathbf{H}^H \mathbf{H} \mathbf{d} \mathbf{F} + \frac{\rho}{P_n} \left(\mathbf{H}^H \mathbf{H} \mathbf{F} \left(\mathbf{I}_{N_s} + \frac{\rho}{P_n} \mathbf{F}^H \mathbf{H}^H \mathbf{H} \mathbf{F} \right)^{-1} \right)^T d \mathbf{F}^* \right\}, \quad (18)$$

from which, using ([22], Table 3.2), allows us to directly obtain (11). Adopting a similar approach, we can write the differential of $f(\mathbf{F}, (\mathbf{I}_{N_{ris}} \otimes \boldsymbol{\theta}^T) \mathbf{t})$ with respect to \mathbf{t} as

$$df = -\text{diag}^T(\mathbf{Z}) d\boldsymbol{\phi} - \text{diag}^T(\mathbf{Z}^H) d\boldsymbol{\phi}^*, \quad (19)$$

where \mathbf{Z} is defined as (13). Considering that $d\boldsymbol{\phi} = (\mathbf{I}_{N_{ris}} \otimes \boldsymbol{\theta}^T) d\mathbf{t}$, we can write

$$df = -2 \text{Re} \left\{ \text{diag}^T(\mathbf{Z}) (\mathbf{I}_{N_{ris}} \otimes \boldsymbol{\theta}^T) \right\} d\mathbf{t}, \quad (20)$$

which, results in the gradient expression in (12). ■

REFERENCES

- [1] S. Mumtaz et al., "Guest Editorial: 6G: The Paradigm for Future Wireless Communications," in *IEEE Wireless Communications*, vol. 29, no. 1, pp. 14-15, February 2022, doi: 10.1109/MWC.2022.9749174.
- [2] M. Matthaiou, O. Yurduseven, H. Q. Ngo, D. Morales-Jimenez, S. L. Cotton and V. F. Fusco, "The Road to 6G: Ten Physical Layer Challenges for Communications Engineers," *IEEE Communications Magazine*, vol. 59, no. 1, pp. 64-69, January 2021, doi: 10.1109/MCOM.001.2000208.
- [3] C. Pan et al., "Reconfigurable Intelligent Surfaces for 6G Systems: Principles, Applications, and Research Directions," in *IEEE Communications Magazine*, vol. 59, no. 6, pp. 14-20, June 2021, doi: 10.1109/MCOM.001.2001076.
- [4] E. Basar, M. Di Renzo, J. De Rosny, M. Debbah, M. -S. Alouini and R. Zhang, "Wireless Communications Through Reconfigurable Intelligent Surfaces," in *IEEE Access*, vol. 7, pp. 116753-116773, 2019, doi: 10.1109/ACCESS.2019.2935192.
- [5] M. Di Renzo et al., "Smart Radio Environments Empowered by Reconfigurable Intelligent Surfaces: How It Works, State of Research, and The Road Ahead," *IEEE Journal on Selected Areas in Communications*, vol. 38, no. 11, pp. 2450-2525, Nov. 2020, doi: 10.1109/JSAC.2020.3007211.
- [6] Y. Liu et al., "Reconfigurable Intelligent Surfaces: Principles and Opportunities," in *IEEE Communications Surveys & Tutorials*, vol. 23, no. 3, pp. 1546-1577, thirdquarter 2021, doi: 10.1109/COMST.2021.3077737.
- [7] J. Praia, J.P. Pavia, N. Souto, M. Ribeiro, "Phase Shift Optimization Algorithm for Achievable Rate Maximization in Reconfigurable Intelligent Surface-Assisted THz Communications," *Electronics*, 11, 18, 2022, doi:10.3390/electronics11010018.
- [8] X. Yu, D. Xu, and R. Schober, "Optimal beamforming for MISO communications via intelligent reflecting surfaces," in *Proc. IEEE 21st Int. Workshop Signal Process. Adv. Wireless Comm. (SPAWC)*, 2020, pp. 1-5.
- [9] N. S. Perović, L. -N. Tran, M. Di Renzo and M. F. Flanagan, "Achievable Rate Optimization for MIMO Systems With Reconfigurable Intelligent Surfaces," in *IEEE Transactions on Wireless Communications*, vol. 20, no. 6, pp. 3865-3882, June 2021, doi: 10.1109/TWC.2021.3054121.
- [10] B. Ning, Z. Chen, W. Chen, and J. Fang, "Beamforming optimization for intelligent reflecting surface assisted MIMO: A sum-path-gain maximization approach," *IEEE Wireless Commun. Lett.*, vol. 9, no. 7, pp. 1105-1109, Jul. 2020.
- [11] Q. Wu and R. Zhang, "Towards Smart and Reconfigurable Environment: Intelligent Reflecting Surface Aided Wireless Network," in *IEEE Communications Magazine*, vol. 58, no. 1, pp. 106-112, January 2020, doi: 10.1109/MCOM.001.1900107.
- [12] Q. Wu and R. Zhang, "Beamforming Optimization for Wireless Network Aided by Intelligent Reflecting Surface With Discrete Phase Shifts," in *IEEE Transactions on Communications*, vol. 68, no. 3, pp. 1838-1851, March 2020, doi: 10.1109/TCOMM.2019.2958916.
- [13] H. Zhang, B. Di, L. Song and Z. Han, "Reconfigurable Intelligent Surfaces Assisted Communications With Limited Phase Shifts: How Many Phase Shifts Are Enough?," in *IEEE Transactions on Vehicular Technology*, vol. 69, no. 4, pp. 4498-4502, April 2020, doi: 10.1109/TVT.2020.2973073.
- [14] J. Sanchez, E. Bengtsson, F. Rusek, J. Flordelis, K. Zhao and F. Tufvesson, "Optimal, Low-Complexity Beamforming for Discrete Phase Reconfigurable Intelligent Surfaces," in *Proc. IEEE Global Communications Conference (GLOBECOM)*, 2021, pp. 01-06, doi: 10.1109/GLOBECOM46510.2021.9685226.
- [15] J. Dai, Y. Wang, C. Pan, K. Zhi, H. Ren and K. Wang, "Reconfigurable Intelligent Surface Aided Massive MIMO Systems With Low-Resolution DACs," in *IEEE Communications Letters*, vol. 25, no. 9, pp. 3124-3128, Sept. 2021, doi: 10.1109/LCOMM.2021.3097208.
- [16] A. Beck, *First-Order Methods in Optimization* (MOS-SIAM Series on Optimization). Philadelphia, PA, USA: SIAM, 2017.
- [17] N. Parikh and S. P. Boyd, "Proximal algorithms," *Found. Trends Optim.*, vol. 1, no. 3, pp. 123-231, 2014.
- [18] Y. Xu and W. Yin, "A globally convergent algorithm for nonconvex optimization based on block coordinate update," *J. Sci. Comput.*, vol. 72, no. 2, pp. 700-734, Aug. 2017.
- [19] W. Wang and M. Á. Carreira-Perpiñán, "Projection onto the probability simplex: An efficient algorithm with a simple proof, and an application," 2013, *arXiv:1309.1541*. [Online]. Available: <http://arxiv.org/abs/1309.1541>
- [20] E. E. Bahingayi and K. Lee, "Low-Complexity Beamforming Algorithms for IRS-Aided Single-User Massive MIMO mmWave Systems," in *IEEE Transactions on Wireless Communications*, doi: 10.1109/TWC.2022.3174154.
- [21] Y. Xing, T. S. Rappaport and A. Ghosh, "Millimeter Wave and Sub-THz Indoor Radio Propagation Channel Measurements, Models, and Comparisons in an Office Environment," in *IEEE Communications Letters*, vol. 25, no. 10, pp. 3151-3155, Oct. 2021, doi: 10.1109/LCOMM.2021.3088264.
- [22] A. Hjørungnes, *Complex-Valued Matrix Derivatives With Applications in Signal Processing and Communications*. Cambridge, U.K.: Cambridge Univ. Press, 2011.